

# Spin-Orbit Misalignment of Merging Black-Hole Binaries with Tertiary Companions

Bin Liu<sup>1</sup> and Dong Lai<sup>2</sup>

<sup>1</sup> *Shanghai Astronomical Observatory, Chinese Academy of Sciences, 80 Nandan Road, Shanghai 200030, China and*

<sup>2</sup> *Cornell Center for Astrophysics and Planetary Science, Cornell University, Ithaca, NY 14853, USA*

We study the effect of external companion on the orbital and spin evolution of merging black-hole (BH) binaries. An sufficiently close by and inclined companion can excite Lidov-Kozai (LK) eccentricity oscillations in the binary, thereby shortening its merger time. During such LK-enhanced orbital decay, the spin axis of the BH generally exhibits chaotic evolution, leading to a wide range ( $0^\circ$ – $180^\circ$ ) of final spin-orbit misalignment angle from an initially aligned configuration. For systems that do not experience eccentricity excitation, only modest ( $\lesssim 20^\circ$ ) spin-orbit misalignment can be produced, and we derive an analytic expression for the final misalignment using the principle of adiabatic invariance. The spin-orbit misalignment directly impacts the gravitational waveform, and can be used to constrain the formation scenarios of BH binaries and dynamical influences of external companions.

*Introduction.*—The recent breakthrough in the detection of gravitational waves (GWs) from merging black hole (BH) binaries by advanced LIGO [1–3] has generated renewed interest in understanding the formation of compact BH binaries. A number of formation channels have been studied, ranging from the evolution of massive stellar binaries [4–8] and triples [9, 10] in the galactic fields, to dynamical interactions in galactic nuclei [11, 12] and in the dense core of globular clusters [13–15].

Because of the uncertainties associated with various formation channels (e.g., common envelope evolution in the standard binary channel), it is difficult to distinguish the different formation mechanisms based on BH mass measurement alone. The detection of eccentric systems would obviously indicates some dynamical processes at work (e.g., [9, 11]). However, because of the efficient eccentricity damping by gravitational radiation, the vast majority of compact binaries will likely be circular when entering the LIGO sensitivity band regardless of the formation channels. It has been suggested that the BH spin and the spin-orbit misalignment angle may be an important discriminant. In particular, the spin-orbit misalignment directly impacts the projected spin parameter of the merging binaries,

$$\chi_{\text{eff}} = \frac{m_1 \mathbf{a}_1 + m_2 \mathbf{a}_2}{m_1 + m_2} \cdot \hat{\mathbf{L}}, \quad (1)$$

(where  $m_{1,2}$  are the BH masses,  $\mathbf{a}_{1,2} = c\mathbf{S}_{1,2}/(Gm_{1,2}^2)$  are the dimensionless BH spins, and  $\hat{\mathbf{L}}$  is the unit orbital angular momentum vector), which can be measured from the phase evolution of GWs [2, 3].

In this paper, we study the merger and spin-orbit misalignment of BH binaries in the presence of tertiary companion. Such triple BH systems could be a direct product of massive triple stars in the galactic field [9, 10], or could be produced dynamically in a dense cluster [13, 14, 16]. For binaries formed near the center of a galaxy, the third body could be a supermassive BH [11, 12].

It is well known that a tertiary body on an inclined orbit can accelerate the decay of an inner binary by inducing Lidov-Kozai (LK) eccentricity/inclination

oscillations [17, 18]. This has been studied before in the contexts of supermassive BH binary merger [19] and stellar mass BH binaries (e.g., [9, 13, 20, 21]). We focus on the latter in this paper. We show that as the BH binary undergoes LK-enhanced decay from a wide orbit and eventually enters the LIGO band, the spin axis of individual BHs can experience chaotic evolution, so that a significant spin-orbit misalignment can be produced prior to merger even for binaries formed with zero initial misalignment. We derive relevant analytic relations and quantify how the final spin-orbit misalignment angle depends on various parameters of the system (binary and external companion).

*Setup and Orbital Evolution.*—Consider a hierarchical triple system, consisting of an inner BH binary with masses  $m_1$ ,  $m_2$  and a relatively distant companion of mass  $m_3$ . The reduced mass for the inner binary is  $\mu_{\text{in}} \equiv m_1 m_2 / m_{12}$ , with  $m_{12} \equiv m_1 + m_2$ . Similarly, the outer binary has  $\mu_{\text{out}} \equiv (m_{12} m_3) / m_{123}$  with  $m_{123} \equiv m_{12} + m_3$ . The orbital semimajor axes and eccentricities are denoted by  $a_{\text{in,out}}$  and  $e_{\text{in,out}}$ , respectively. The orbital angular momenta of the inner and outer binaries are

$$\mathbf{L}_{\text{in}} = L_{\text{in}} \hat{\mathbf{L}}_{\text{in}} = \mu_{\text{in}} \sqrt{G m_{12} a_{\text{in}} (1 - e_{\text{in}}^2)} \hat{\mathbf{L}}_{\text{in}}, \quad (2)$$

$$\mathbf{L}_{\text{out}} = L_{\text{out}} \hat{\mathbf{L}}_{\text{out}} = \mu_{\text{out}} \sqrt{G m_{123} a_{\text{out}} (1 - e_{\text{out}}^2)} \hat{\mathbf{L}}_{\text{out}} \quad (3)$$

where  $\hat{\mathbf{L}}_{\text{in,out}}$  are unit vectors. The relative inclination between  $\hat{\mathbf{L}}_{\text{in}}$  and  $\hat{\mathbf{L}}_{\text{out}}$  is denoted by  $I$ . For convenience of notation, we will frequently omit the subscript “in”.

The merger time due to GW radiation of an isolated binary with initial  $a_0$  and  $e_0 = 0$  is given by

$$T_{\text{m},0} = \frac{5c^5 a_0^4}{256G^3 m_{12}^2 \mu} \simeq 10^{10} \left( \frac{60M_\odot}{m_{12}} \right)^2 \left( \frac{15M_\odot}{\mu} \right) \left( \frac{a_0}{0.202\text{AU}} \right)^4 \text{ yrs.} \quad (4)$$

A sufficiently inclined external companion can raise the binary eccentricity through Lidov-Kozai oscillations, thereby reducing the merger time or making an otherwise

non-merging binary merge within  $10^{10}$  years. To study the evolution of merging BH binary under the influence of a companion, we use the secular equations to the octupole level in terms of the angular momentum  $\mathbf{L}$  and eccentricity  $\mathbf{e}$  vectors:

$$\frac{d\mathbf{L}}{dt} = \frac{d\mathbf{L}}{dt}\bigg|_{\text{LK}} + \frac{d\mathbf{L}}{dt}\bigg|_{\text{GW}}, \quad (5)$$

$$\frac{d\mathbf{e}}{dt} = \frac{d\mathbf{e}}{dt}\bigg|_{\text{LK}} + \frac{d\mathbf{e}}{dt}\bigg|_{\text{GR}} + \frac{d\mathbf{e}}{dt}\bigg|_{\text{GW}}. \quad (6)$$

Here the ‘‘Lidov-Kozai’’ (LK) terms are given explicitly in [22] (we also evolve  $\mathbf{L}_{\text{out}}$  and  $\mathbf{e}_{\text{out}}$ ), and the associated timescale of LK oscillation is

$$t_{\text{LK}} = \frac{1}{n} \frac{m_{12}}{m_3} \left( \frac{a_{\text{out,eff}}}{a} \right)^3, \quad (7)$$

where  $n = \sqrt{Gm_{12}/a^3}$  is the mean motion of the inner binary and  $a_{\text{out,eff}} \equiv a_{\text{out}} \sqrt{1 - e_{\text{out}}^2}$ . General Relativity (post-1 Newtonian correction) induces pericenter precession

$$\frac{d\mathbf{e}}{dt}\bigg|_{\text{GR}} = \Omega_{\text{GR}} \hat{\mathbf{L}} \times \mathbf{e}, \quad (8)$$

with the precession rate given by

$$\Omega_{\text{GR}} = \frac{3Gnm_{12}}{c^2 a (1 - e^2)}. \quad (9)$$

GW emission (post-2.5 Newtonian effect) causes orbital decay and circularization, with

$$\frac{d\mathbf{L}}{dt}\bigg|_{\text{GW}} = -\frac{32}{5} \frac{G^{7/2}}{c^5} \frac{\mu^2 m_{12}^{5/2}}{a^{7/2}} \frac{(1 + 7e^2/8)}{(1 - e^2)^2} \hat{\mathbf{L}}, \quad (10)$$

$$\frac{d\mathbf{e}}{dt}\bigg|_{\text{GW}} = -\frac{304}{15} \frac{G^3}{c^5} \frac{\mu m_{12}^2}{a^4} \frac{(1 + 121e^2/304)}{(1 - e^2)^{5/2}} \mathbf{e}. \quad (11)$$

We do not consider extreme eccentricity excitation due to non-secular effects in this paper [9, 21].

The top three panels of Fig. 1 show an example of the orbital evolution of a BH binary with an inclined companion (initial  $I_0 = 80^\circ$ ). We see that the inner binary undergoes cyclic excursions to maximum eccentricity  $e_{\text{max}}$ , with accompanying oscillations in the inclination  $I$ . As the binary decays, the range of eccentricity oscillations shrinks. Eventually the oscillations freeze and the binary experiences ‘‘pure’’ orbital decay/circularization governed by GW dissipation.

*Eccentricity Excitation and Merger Time.* In the quadrupole approximation, the maximum eccentricity  $e_{\text{max}}$  attained in the LK oscillations (starting from an initial  $I_0$  and  $e_0 \simeq 0$ ) can be calculated analytically using energy and angular momentum conservation, according to the equation [23]

$$\frac{3}{8} \frac{j_{\text{min}}^2 - 1}{j_{\text{min}}^2} \left[ 5 \left( \cos I_0 + \frac{\eta}{2} \right)^2 - \left( 3 + 4\eta \cos I_0 + \frac{9}{4} \eta^2 \right) j_{\text{min}}^2 \right] + \varepsilon_{\text{GR}} (1 - j_{\text{min}}^{-1}) = 0, \quad (12)$$

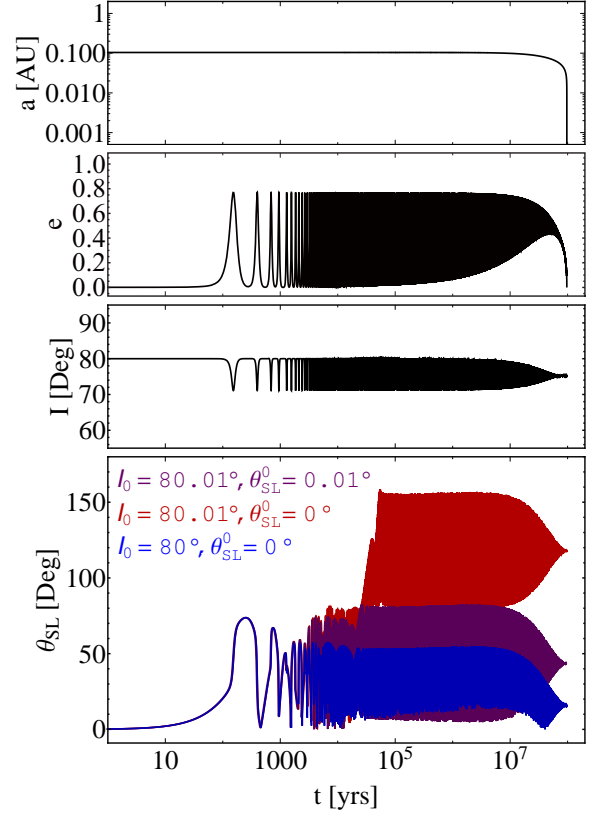


FIG. 1: Sample orbital and spin evolution of a BH binary system with a tertiary companion. The top three panels show the semimajor axis, eccentricity and inclination (relative to  $\hat{\mathbf{L}}_{\text{out}}$ ) of the inner BH binary, and the bottom panel shows the spin-orbit misalignment (the angle between  $\mathbf{S}_1$  and  $\mathbf{L}$ ). The parameters are  $m_1 = m_2 = m_3 = 30M_\odot$ ,  $a_{\text{out}} = 3\text{AU}$ ,  $e_{\text{out}} = 0$ , and the initial  $a_0 = 0.1\text{AU}$ ,  $e_0 = 0.001$ ,  $I_0 = 80^\circ$  and  $\theta_{\text{SL}}^0 = 0^\circ$ . For this example, the octupole effect is absent. In the bottom panel, the results for slightly different values of  $I_0$  and  $\theta_{\text{SL}}^0$  (as indicated) are plotted, showing a strong dependence of the final  $\theta_{\text{SL}}$  on the initial conditions.

where  $j_{\text{min}} \equiv \sqrt{1 - e_{\text{max}}^2}$ ,  $\eta \equiv (L/L_{\text{out}})_{e=0}$  and  $\varepsilon_{\text{GR}}$  is given by

$$\varepsilon_{\text{GR}} = t_{\text{LK}} \Omega_{\text{GR}} \bigg|_{e=0} = \frac{3Gm_{12}^2 a_{\text{out,eff}}^3}{c^2 a^4 m_3} \simeq 0.96 \left( \frac{m_{12}}{60M_\odot} \right)^2 \left( \frac{m_3}{30M_\odot} \right)^{-1} \left( \frac{a_{\text{out,eff}}}{3\text{AU}} \right)^3 \left( \frac{a}{0.1\text{AU}} \right)^{-4} \quad (13)$$

Note that in the limit of  $\eta \rightarrow 0$  and  $\varepsilon_{\text{GR}} \rightarrow 0$ , Eq. (12) yields the well-known relation  $e_{\text{max}} = \sqrt{1 - (5/3) \cos^2 I_0}$ . The maximum possible  $e_{\text{max}}$  for all values of  $I_0$ , called  $e_{\text{lim}}$ , is given by

$$\frac{3}{8} (j_{\text{lim}}^2 - 1) \left[ -3 + \frac{\eta^2}{4} \left( \frac{4}{5} j_{\text{lim}}^2 - 1 \right) \right] + \varepsilon_{\text{GR}} (1 - j_{\text{lim}}^{-1}) = 0, \quad (14)$$

and is reached at  $\cos I_0 = (\eta/10)(4j_{\text{lim}}^2 - 5)$ . Eccentricity excitation ( $e_{\text{max}} \geq 0$ ) occurs within a window of inclina-

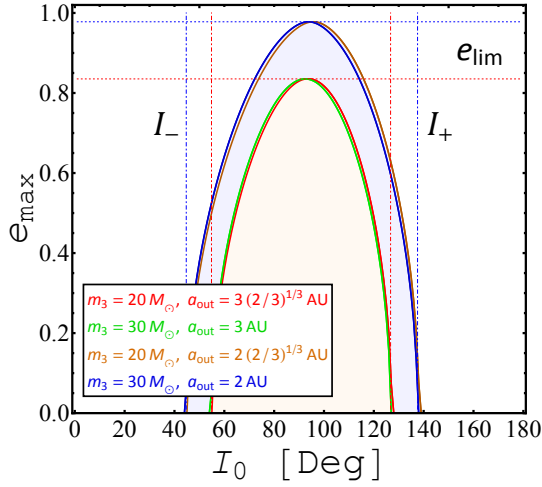


FIG. 2: The maximum eccentricity of the inner BH binary versus the initial inclination  $I_0$  of the tertiary companion, calculated using Eq. (12). The inner binary has  $m_1 = m_2 = 30M_\odot$ ,  $a = 0.1\text{AU}$ , and initial  $e_0 \simeq 0$ . The companion has a circular orbit and its mass and semimajor axis are as labeled. The  $e_{\text{max}}(I_0)$  curve depends mainly on  $m_3/a_{\text{out}}^3$ . The horizontal ( $e_{\text{lim}}$ ) and vertical ( $I_\pm$ ) lines are given by Eqs. (14) and (15), respectively.

tions  $(\cos I_0)_- \leq \cos I_0 \leq (\cos I_0)_+$ , where [23]

$$(\cos I_0)_\pm = \frac{1}{10} \left( -\eta \pm \sqrt{\eta^2 + 60 - \frac{80}{3}\varepsilon_{\text{GR}}} \right). \quad (15)$$

This window vanishes when

$$\varepsilon_{\text{GR}} \geq \frac{9}{4} + \frac{3}{80}\eta^2 \quad (\text{no eccentricity excitation}). \quad (16)$$

Figure 2 shows some examples of the  $e_{\text{max}}(I_0)$  curves. For  $\eta \lesssim 1$ , these curves depend mainly on  $m_3/a_{\text{out,eff}}^3$  (for given inner binary parameters). As  $\varepsilon_{\text{GR}}$  increases (with decreasing  $m_3/a_{\text{out,eff}}^3$ ), the LK window shrinks and  $e_{\text{lim}}$  decreases. Eccentricity excitation is suppressed (for all  $I_0$ 's) when Eq. (16) is satisfied.

For systems with  $m_1 \neq m_2$  and  $e_{\text{out}} \neq 0$ , so that

$$\varepsilon_{\text{oct}} \equiv \frac{m_1 - m_2}{m_{12}} \left( \frac{a}{a_{\text{out}}} \right) \frac{e_{\text{out}}}{1 - e_{\text{out}}^2} \quad (17)$$

is non-negligible, the octupole effect may become important (e.g. [24, 25]). This tends to widen the inclination window for large eccentricity excitation. However, the analytic expression for  $e_{\text{lim}}$  given by Eq. (14) remains valid even for  $\varepsilon_{\text{oct}} \neq 0$  [22, 26]. Therefore Eq. (16) still provides a good criterion for “negligible eccentricity excitation” (note that when  $\varepsilon_{\text{oct}} \neq 0$ , the inner binary cannot be exactly circular; e.g., [26, 27]).

Eccentricity excitation leads to a shorter binary merger time  $T_m$  compared to the circular merger time  $T_{m,0}$  (Fig. 3). We compute  $T_m$  by integrating the secular evolution equations of the BH triples with a range of  $I_0$ .

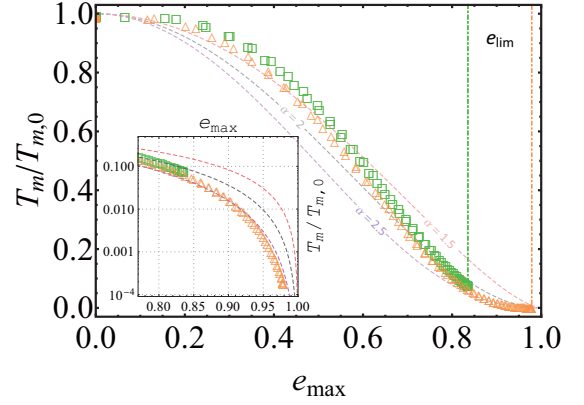


FIG. 3: The binary merger time  $T_m$  (in units of  $T_{m,0}$ ; Eq. 4) as a function of the maximum eccentricity induced by a tertiary companion. The BH masses are  $m_1 = m_2 = m_3 = 30M_\odot$ , and the inner and outer orbits are initially circular. We consider two sets of initial semimajor axes:  $a_0 = 0.1\text{AU}$ ,  $a_{\text{out}} = 3\text{AU}$  (orange) and  $a_0 = 0.2\text{AU}$ ,  $a_{\text{out}} = 5\text{AU}$  (green). Here  $T_m$  is computed numerically by integrating the secular evolution equations with different  $I_0$ 's, and  $e_{\text{max}}$  is calculated using Eq. (12). The decreasing trend of  $T_m/T_{m,0}$  as a function of  $e_{\text{max}}$  can be approximated by  $(1 - e_{\text{max}}^2)^\alpha$  (dashed lines). The inset shows a zoomed-in portion of large  $e_{\text{max}}$ 's.

Each  $I_0$  run has a corresponding  $e_{\text{max}}$ , which can be calculated using Eq. (12). We see that in general  $T_m/T_{m,0}$  can be approximated by  $(1 - e_{\text{max}}^2)^\alpha$ , with  $\alpha \simeq 1.5, 2$  and  $2.5$  for  $e_{\text{max}} = (0, 0.6)$ ,  $(0.6, 0.8)$  and  $(0.8, 0.95)$ , respectively.

*Spin-Orbit Coupling.*— We now study how the BH spin evolves during the binary merger. We consider only  $\mathbf{S}_1 = S_1 \hat{\mathbf{S}}_1$  (where  $\hat{\mathbf{S}}_1$  is the unit vector), and neglect spin-spin interactions. (The evolution of  $\mathbf{S}_2$  can of course be studied similarly.) The evolution equation for  $\hat{\mathbf{S}}_1$  is [28]

$$\frac{d\hat{\mathbf{S}}_1}{dt} = \Omega_{\text{dS}} \hat{\mathbf{L}} \times \hat{\mathbf{S}}_1, \quad (18)$$

with the orbital-averaged de Sitter precession rate

$$\Omega_{\text{dS}} = \frac{3Gn(m_2 + \mu/3)}{2c^2a(1 - e^2)}. \quad (19)$$

Note that there is a back-reaction torque from  $\mathbf{S}_1$  on  $\mathbf{L}$ ; this can be safely neglected since  $L \gg S_1$ . We also neglect the (much slower) de Sitter precession of  $\hat{\mathbf{S}}_1$  induced by  $m_3$ .

Before presenting our numerical results, it is useful to note the different regimes for the evolution of the spin-orbit misalignment angle  $\theta_{\text{SL}}$  (the angle between  $\mathbf{S}_1$  and  $\mathbf{L}$ ). In general, the inner binary axis  $\hat{\mathbf{L}}$  precesses (and nutates when  $e \neq 0$ ) around the total angular momentum  $\mathbf{J} = \mathbf{L} + \mathbf{L}_{\text{out}}$  (recall that  $S_1, S_2 \ll L$ , and  $\mathbf{J}$  is constant in the absence of GW dissipation). The related precession rate  $\Omega_L$  is of order  $t_{\text{LK}}^{-1}$  at  $e \sim 0$  (Eq. 21), but increases with  $e$ . Depending on the ratio of  $\Omega_{\text{dS}}$  and  $\Omega_L$ , we expect three possible spin behaviors: (i) For

$\Omega_L \gg \Omega_{\text{ds}}$  (“nonadiabatic”), the spin axis  $\hat{\mathbf{S}}_1$  cannot “keep up” with the rapidly changing  $\hat{\mathbf{L}}$ , and thus effectively precesses around  $\hat{\mathbf{J}}$ , keeping  $\theta_{\text{SJ}} \equiv \cos^{-1}(\hat{\mathbf{S}}_1 \cdot \hat{\mathbf{J}}) \simeq$  constant. (ii) For  $\Omega_{\text{ds}} \gg \Omega_L$  (“adiabatic”),  $\hat{\mathbf{S}}_1$  closely “follows”  $\hat{\mathbf{L}}$ , maintaining an approximately constant  $\theta_{\text{SL}}$ . (iii) For  $\Omega_{\text{ds}} \sim \Omega_L$  (“trans-adiabatic”), the spin evolution can be chaotic due to overlapping resonances. Since both  $\Omega_{\text{ds}}$  and  $\Omega_L$  depend on  $e$  during the LK cycles, the precise transitions between these regimes can be fuzzy [29–32].

For circular orbits ( $e = 0$ ), the precession of  $\hat{\mathbf{L}}$  is governed by the equation

$$\left. \frac{d\hat{\mathbf{L}}}{dt} \right|_{\text{LK}, e=0} = -\Omega_L \hat{\mathbf{L}}_{\text{out}} \times \hat{\mathbf{L}} = -\Omega'_L \hat{\mathbf{J}} \times \hat{\mathbf{L}}, \quad (20)$$

where  $\hat{\mathbf{J}}$  is the unit vector along  $\mathbf{J} = \mathbf{L} + \mathbf{L}_{\text{out}}$ , and

$$\Omega_L = \frac{3}{4t_{\text{LK}}}(\hat{\mathbf{L}} \cdot \hat{\mathbf{L}}_{\text{out}}), \quad \Omega'_L = \Omega_L \frac{J}{L_{\text{out}}}. \quad (21)$$

We can define an “adiabaticity parameter”

$$\begin{aligned} \mathcal{A} \equiv \left( \frac{\Omega_{\text{ds}}}{\Omega_L} \right)_{e, I=0} &\simeq 0.37 \left[ \frac{(m_2 + \mu/3)}{35M_\odot} \right] \left( \frac{m_{12}}{60M_\odot} \right) \\ &\times \left( \frac{m_3}{30M_\odot} \right)^{-1} \left( \frac{a_{\text{out, eff}}}{3\text{AU}} \right)^3 \left( \frac{a}{0.1\text{AU}} \right)^{-4}. \end{aligned} \quad (22)$$

As the binary orbit decays, the system may transition from “non-adiabatic” ( $\mathcal{A} \ll 1$ ) at large  $a$ ’s to “adiabatic” ( $\mathcal{A} \gg 1$ ) at small  $a$ ’s, where the final spin-orbit misalignment angle  $\theta_{\text{SL}}^f$  is “frozen”. Note that  $\mathcal{A}$  is directly related to  $\varepsilon_{\text{GR}}$  by

$$\frac{\mathcal{A}}{\varepsilon_{\text{GR}}} = \frac{2}{3} \frac{m_2 + \mu/3}{m_{12}}. \quad (23)$$

Thus, when the initial value of  $\varepsilon_{\text{GR}}$  (at  $a = a_0$ ) satisfies  $\varepsilon_{\text{GR},0} \lesssim 9/4$  (a necessary condition for LK eccentricity excitation; see Eq. 16), we also have  $\mathcal{A}_0 \lesssim (3m_2 + \mu)/(2m_{12})$ . This implies that any system that experiences enhanced orbital decay due to LK oscillations must go through the “trans-adiabatic” regime and therefore possibly chaotic spin evolution.

The bottom panel of Fig. 1 shows a representative example of the evolution of the misalignment angle as the BH binary undergoes LK-enhanced orbital decay. We see that the BH spin axis can exhibit complex evolution even though the orbital evolution is “regular”. In particular,  $\theta_{\text{SL}}$  evolves in a chaotic way, with the final value  $\theta_{\text{SL}}^f$  depending sensitively on the initial conditions (the precise initial  $\theta_{\text{SL}}$  and  $I_0$ ). Also note that retrograde spin ( $\theta_{\text{SL}}^f > 90^\circ$ ) can be produced even though the binary always remains prograde with respect to the outer companion ( $I < 90^\circ$ ). These behaviors are qualitatively similar to the chaotic evolution of stellar spin driven by Newtonian spin-orbit coupling with a giant planet undergoing high-eccentricity migration [29–32].

We carry out a series of numerical integrations, evolving the orbit of the merging BH binary with a tertiary companion, along with spin-orbit coupling, to determine  $\theta_{\text{SL}}^f$  for various triple parameters. In our “population synthesis” study, we consider initial conditions such that  $\hat{\mathbf{S}}_1$  is parallel to  $\hat{\mathbf{L}}$ , the binary inclinations are isotropically distributed (uniform distribution in  $\cos I_0$ ), and the orientations of  $\mathbf{e}$  and  $\mathbf{e}_{\text{out}}$  (for systems with  $e_{\text{out}} \neq 0$ ) are random. All initial systems satisfy the criterion of dynamical stability for triples [33].

Figure 4 shows our results for systems with equal masses,  $e_{\text{out}} = 0$  (so that the octupole effect vanishes), and several values of  $a_{\text{out}}$ . We see that when the eccentricity of the inner binary is excited ( $I_0$  lies in the LK window), a wide range of  $\theta_{\text{SL}}^f$  is generated, including appreciable fraction of retrograde ( $\theta_{\text{SL}}^f > 90^\circ$ ) systems (see the  $a_{\text{out}} = 3$  AU case, for which  $e_{\text{lim}} = 0.84$ ). The “memory” of chaotic spin evolution is evident, as slightly different initial inclinations lead to vastly different  $\theta_{\text{SL}}^f$ . The regular behavior of  $\theta_{\text{SL}}^f$  around  $I_0 = 90^\circ$  (again for the  $a_{\text{out}} = 3$  AU case) is intriguing, but may be understood using the theory developed in Ref. [32]. For systems with no eccentricity excitation,  $\theta_{\text{SL}}^f$  varies regularly as a function of  $I_0$  – this can be calculated analytically (see below).

Figure 5 shows our results for systems with  $m_1 \neq m_2$  and  $e_{\text{out}} \neq 0$ , for which octupole terms may affect the orbital evolution. We see that eccentricity excitation and the corresponding reduction in  $T_{\text{m}}$  occur outside the analytic (quadrupole) LK window (see the  $e_{\text{out}} = 0.8$  case, for which  $e_{\text{lim}} = 0.66$ ). As in the equal-mass case (Fig. 4), a wide range of  $\theta_{\text{SL}}^f$  values are produced whenever eccentricity excitation occurs. A larger fraction (23%) of systems attain retrograde spin ( $\theta_{\text{SL}}^f > 90^\circ$ ). Again, for systems with negligible eccentricity excitation,  $\theta_{\text{SL}}^f$  behaves regularly as a function of  $I_0$  and agrees with the analytic result (the “fuzziness” of the numerical result in this regime is likely due to the very small eccentricity of the inner binary; see [27]).

*Analytical Calculation of  $\theta_{\text{SL}}^f$  for Circular Binaries.* — If the inner binary experiences no eccentricity excitation and remains circular throughout the orbital decay, the final spin-orbit misalignment can be calculated analytically using the principle of adiabatic invariance.

Equation (20) shows that  $\hat{\mathbf{L}}$  rotates around the  $\hat{\mathbf{J}}$  axis at the rate  $(-\Omega'_L)$ . In this rotating frame, the spin evolution equation (18) transforms to

$$\left( \frac{d\hat{\mathbf{S}}_1}{dt} \right)_{\text{rot}} = \boldsymbol{\Omega}_{\text{eff}} \times \hat{\mathbf{S}}_1, \quad (24)$$

where the effective rotation rate vector is

$$\boldsymbol{\Omega}_{\text{eff}} \equiv \Omega_{\text{ds}} \hat{\mathbf{L}} + \Omega'_L \hat{\mathbf{J}} = (\Omega_{\text{ds}} + \eta \Omega_L) \hat{\mathbf{L}} + \Omega_L \hat{\mathbf{L}}_{\text{out}}. \quad (25)$$

Note that in the absence of GW dissipation,  $\hat{\mathbf{L}}$  and  $\hat{\mathbf{L}}_{\text{out}}$  are constants (in the rotating frame), and thus  $\hat{\mathbf{S}}_1$  precesses with a constant  $\boldsymbol{\Omega}_{\text{eff}}$ . The relative inclination be-

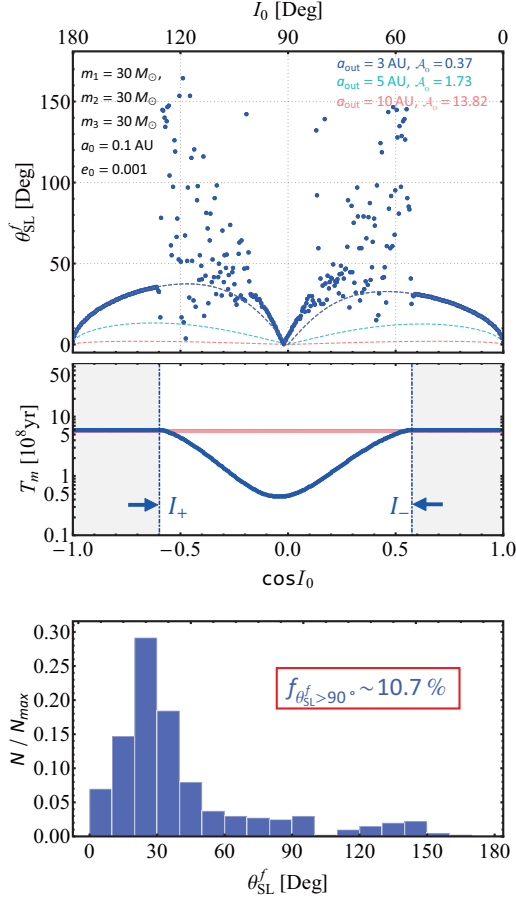


FIG. 4: Final spin-orbit misalignment angle (top panel) and merger time (middle panel) as a function of the initial inclination for equal mass triple systems with different outer semimajor axes (as labeled). The inner binary has fixed initial  $a_0 = 0.1 \text{ AU}$  and  $e_0 \simeq 0$ , and  $e_{\text{out}} = 0$  for the outer binary. In the top panel, the dots are the result of numerical integration for the  $a_{\text{out}} = 3 \text{ AU}$  system (a total of 400 runs on a uniform  $\cos I_0$  grid), and the dashed curves are the analytical results for circular orbits, as given by Eqs. (28) and (29). The initial value of the adiabaticity parameter  $\mathcal{A}_0$  (Eq. 22 with  $a = a_0$ ) is also given. The vertical lines ( $I_{\pm}$ ) shown in the middle panel correspond to the LK window of eccentricity excitation (Eq. 15). The bottom panel shows the distribution of the final spin-orbit misalignment angle for the system with  $a_{\text{out}} = 3 \text{ AU}$ .

tween  $\mathbf{\Omega}_{\text{eff}}$  and  $\hat{\mathbf{L}}$  is given by

$$\tan \theta_{\text{eff,L}} = \frac{\Omega_L \sin I}{\Omega_{\text{ds}} + (\eta + \cos I)\Omega_L}. \quad (26)$$

Now if we include GW dissipation,  $\hat{\mathbf{L}} \cdot \hat{\mathbf{L}}_{\text{out}} = \cos I$  is exactly conserved, and  $\mathbf{\Omega}_{\text{eff}}$  becomes a slowly changing vector. When the rate of change of  $\mathbf{\Omega}_{\text{eff}}$  is much smaller than  $|\mathbf{\Omega}_{\text{eff}}|$ , the angle between  $\mathbf{\Omega}_{\text{eff}}$  and  $\hat{\mathbf{S}}_1$  is adiabatic invariant, i.e.

$$\theta_{\text{eff,S}_1} \simeq \text{constant} \quad (\text{adiabatic invariant}). \quad (27)$$

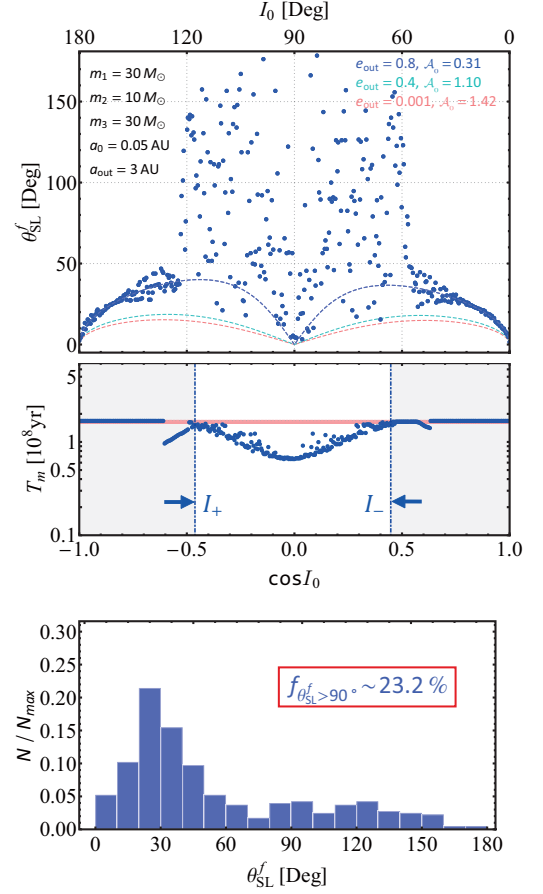


FIG. 5: Same as Fig.4, but for unequal masses and non-circular outer orbits (as labeled). The dots in the top panel are numerical results for the  $e_{\text{out}} = 0.8$  system (a total of 400 runs on a uniform  $\cos I_0$  grid), and the bottom panel shows the distribution of  $\theta_{\text{SL}}^f$  for such a system.

This adiabatic invariance requires  $|d\mathbf{\Omega}_{\text{eff}}/dt|/|\mathbf{\Omega}_{\text{eff}}| \sim T_{m,0}^{-1} \ll |\mathbf{\Omega}_{\text{eff}}|$ , or  $|\mathbf{\Omega}_{\text{eff}}|T_{m,0} \gg 1$ , which is easily satisfied.

Suppose  $\hat{\mathbf{S}}_1$  and  $\hat{\mathbf{L}}$  are aligned initially, we have  $\theta_{\text{eff,S}_1}^0 = \theta_{\text{eff,L}}^0$  (the superscript 0 denotes initial value). Equation (27) then implies  $\theta_{\text{eff,S}_1} \simeq \theta_{\text{eff,L}}^0$  at all times. After the binary has decayed,  $\eta \rightarrow 0$ ,  $|\Omega_{\text{ds}}| \gg |\Omega_L|$ , and therefore  $\mathbf{\Omega}_{\text{eff}} \simeq \Omega_{\text{ds}}\hat{\mathbf{L}}$ , which implies  $\theta_{\text{SL}}^f \simeq \theta_{\text{eff,S}_1}^0$ . Thus we find

$$\theta_{\text{SL}}^f \simeq \theta_{\text{eff,L}}^0. \quad (28)$$

That is, the final spin-orbit misalignment angle is equal to the initial inclination angle between  $\hat{\mathbf{L}}$  and  $\mathbf{\Omega}_{\text{eff}}$ , obtained by evaluating Eq. (26) at  $a = a_0$ :

$$\tan \theta_{\text{eff,L}}^0 = \frac{\sin I_0}{(\mathcal{A}_0/\cos I_0) + \eta_0 + \cos I_0}. \quad (29)$$

This analytic expression agrees with the numerical results shown in Figs. 4-5 in the appropriate regime. Note that for systems that experience no eccentricity excitation for

all  $I_0$ 's,  $\mathcal{A}_0 \gtrsim (3m_2 + \mu)/(2m_{12}) \sim 1$  (see Eqs. 16 and 23), and thus  $\theta_{\text{SL}}^f \simeq \theta_{\text{eff,L}}^0 \lesssim 20^\circ$ , i.e., only modest spin-orbit misalignment can be generated. For systems with  $\mathcal{A}_0 \gg 1$  (e.g., very distant companion), we have  $\theta_{\text{SL}}^f \ll 1$ .

The above analytical result can be easily generalized to the situation of non-zero initial spin-orbit misalignment. It shows that  $\theta_{\text{SL}}^f \simeq \theta_{\text{SL}}^0$  for  $\mathcal{A}_0 \gg 1$ .

*Summary and Discussion.*— We have studied the effect of external companion on the orbital and spin evolution of merging BH binaries due to gravitational radiation. A sufficiently close by and inclined companion can excite Lidov-Kozai eccentricity oscillation in the binary, shortening its merger time compared to circular orbits [by a factor of  $(1 - e_{\text{max}}^2)^\alpha$ , see Fig. 3]. We find that during the LK-enhanced orbital decay, the spin axis of the BH generally experiences complex, chaotic evolution, with the final spin-orbit misalignment angle  $\theta_{\text{SL}}^f$  depending sensitively on the initial conditions. A wide range of  $\theta_{\text{SL}}^f$  (including  $\theta_{\text{SL}}^f > 90^\circ$ ) can be produced from an initially aligned ( $\theta_{\text{SL}}^0 = 0$ ) configuration (see Figs. 4-5). For systems that do not experience eccentricity excitation (because of relatively low orbital inclinations of the companion or/and suppression by GR-induced precession), modest ( $\lesssim 20^\circ$ ) spin-orbit misalignment can be produced – we have derived an analytic expression for  $\theta_{\text{SL}}^f$  for such systems (Eqs. 28-29). Note that while our

numerical results refer to tertiary stellar-mass companions, our analysis is not restricted to any specific binary formation scenarios, and can be easily adapted to other types of systems (e.g. when the tertiary is a supermassive BH) by applying appropriate scaling relations.

The BH binaries detected by aLIGO so far [2, 3] have relatively small  $\chi_{\text{eff}}$  ( $0.06^{+0.14}_{-0.14}$  for GW150914,  $0.21^{+0.2}_{-0.1}$  for GW151226, and  $-0.12^{+0.21}_{-0.30}$  for GW170104). These small values could be due to the slow rotation of the BHs [34] or spin-orbit misalignments. The latter possibility would imply a dynamical formation channel of the BH binaries (such as exchange interaction in globular clusters [14, 15]) or, as our calculations indicate, dynamical influences of external companions.

*Acknowledgments.*— BL thanks Natalia Storch, Feng Yuan and Xing-Hao Liao for discussions. This work is supported in part by grants from the National Postdoctoral Program for Innovative Talents (No. BX201600179 and No. 2016M601673). DL is supported by NASA grants NNX14AG94G and NNX14AP31G, and a Simons Fellowship in theoretical physics. This work made use of the High Performance Computing Resource in the Core Facility for Advanced Research Computing at Shanghai Astronomical Observatory.

- 
- [1] B. P. Abbott et al. (LIGO Scientific and Virgo Collaboration), Phys. Rev. Lett. **116**, 061102 (2016a).
  - [2] B. P. Abbott et al. (LIGO Scientific and Virgo Collaboration), Phys. Rev. X **6**, 041015 (2016b).
  - [3] B. P. Abbott et al. (LIGO Scientific and Virgo Collaboration), Phys. Rev. Lett. **118**, 221101 (2017).
  - [4] V.M. Lipunov, K.A. Postnov, and M.E. Prokhorov, Astro. Lett. **23**, 492 (1997)
  - [5] K. Belczynski, M. Benacquista, and T. Bulik, Astrophys. J. **725**, 816 (2010)
  - [6] K. Belczynski, D. E. Holz, T. Bulik, and R. O'Shaughnessy, Nature (London) **534**, 512 (2016)
  - [7] I. Mandel and S. E. de Mink, Mon. Not. Roy. Astron. Soc. **458**, 2634 (2016)
  - [8] V.M. Lipunov, et al., Mon. Not. Roy. Astron. Soc. **465**, 3656 (2017)
  - [9] K. Silsbee and S. Tremaine, Astrophys. J. **836**, 39 (2017)
  - [10] F. Antonini, S. Toonen, and A. S. Hamers, Astrophys. J. **841**, 77 (2017)
  - [11] F. Antonini and H.B. Perets, Astrophys. J. **757**, 27 (2012)
  - [12] C. Petrovich and F. Antonini, arXiv:1705.05848
  - [13] M.C. Miller and D.P. Hamilton, Astrophys. J. **576**, 894 (2002)
  - [14] C. L. Rodriguez, et al. Phys. Rev. Lett. **115**, 051101 (2015)
  - [15] S. Chatterjee, C. L. Rodriguez, V. Kalogera, and F. A. Rasio, Astrophys. J. **836**, L26 (2017)
  - [16] F. Antonini and F. A. Rasio, Astrophys. J. **831**, 187 (2016)
  - [17] M. L. Lidov, Planetary and Space Science **9**, 719 (1962)
  - [18] Y. Kozai, Astron. J. **67**, 591 (1962)
  - [19] O. Blaes, M. H. Lee, and A. Socrates, Astrophys. J. **578**, 775 (2002)
  - [20] T. A. Thompson, Astrophys. J. **741**, 82 (2011)
  - [21] F. Antonini, N. Murray, and S. Mikkola, Astrophys. J. **781**, 45 (2014)
  - [22] B. Liu, D. J. Muñoz, and D. Lai, Mon. Not. Roy. Astron. Soc. **447**, 747 (2015)
  - [23] K. R. Anderson, D. Lai, and N. I. Storch, Mon. Not. Roy. Astron. Soc. **467**, 3066 (2017)
  - [24] E. B. Ford, B. Kozinsky, and F. A. Rasio, Astrophys. J. **535**, 385 (2000)
  - [25] S. Naoz, Ann. Rev. Astro. Astrophys. **54**, 441 (2016)
  - [26] K. R. Anderson and D. Lai, arXiv:1706.00084
  - [27] B. Liu, D. Lai and Y-F Yuan, Phys. Rev D **92**, 124048 (2015)
  - [28] B. M. Barker and R. F.O'Connell, Phys. Rev. D **12**, 329 (1975)
  - [29] N. I. Storch, K. R. Anderson, and D. Lai, Science **345**, 1317 (2014)
  - [30] N. I. Storch and D. Lai, Mon. Not. Roy. Astron. Soc. **448**, 1821 (2015)
  - [31] K. R. Anderson, N. I. Storch, and D. Lai, Mon. Not. Roy. Astron. Soc. **456**, 3671 (2016)
  - [32] N. I. Storch, D. Lai and K.R. Anderson, Mon. Not. Roy. Astron. Soc. **465**, 3927 (2017)
  - [33] R. A. Mardling and S.J. Aarseth, Mon. Not. Roy. Astron. Soc. **321**, 398 (2001)
  - [34] M. Zaldarriaga, D. Kushnir and J.A. Kollmeier, arXiv:1702.00885